Electroreduction of Sulfur Dioxide in Some Room-Temperature Ionic Liquids

Laura E. Barrosse-Antle,[†] Debbie S. Silvester,[†] Leigh Aldous,[‡] Christopher Hardacre,[‡] and Richard G. Compton*,[†]

Physical and Theoretical Chemistry Laboratory, University of Oxford, South Parks Road, Oxford OX1 3QZ, United Kingdom, and School of Chemistry and Chemical Engineering/QUILL, Queen's University Belfast, Belfast, Northern Ireland BT9 5AG, United Kingdom

Received: November 15, 2007

The mechanism of sulfur dioxide reduction at a platinum microelectrode was investigated by cyclic voltammetry in several room-temperature ionic liquids (RTILs)—[C_2mim][NTf_2], [C_4mim][BF_4], [C_4mim][NO_3], [C_4mim][PF_6], and [C_6mim][Cl] where [C_2mim] is 1-ethyl-3-methylimidazolium, [C_4mim] is 1-butyl-3-methylimidazolium, [C_6mim] is 1-hexyl-3-methylimidazolium, and [NTf_2] is bis(trifluoromethylsufonyl)imide—with special attention paid to [C_4mim][NO_3] because of the well-defined voltammetry, high solubility, and relatively low diffusion coefficient of SO_2 obtained in that ionic liquid. A cathodic peak is observed in all RTILs between −2.0 and −1.0 V versus a silver quasi-reference electrode. In [C_4mim][NO_3], the peak appears at −1.0 V, and potential step chronoamperometry was used to determine that SO_2 has a very high solubility of 3100 (±450) mM and a diffusion coefficient of 5.0 (±0.8) × 10^{-10} m^2 s^{-1} in that ionic liquid. On the reverse wave, up to four anodic peaks are observed at ca. −0.4, −0.3, −0.2, and 0.2 V in [C_4mim][NO_3]. The cathodic wave is assigned to the reduction of SO_2 to its radical anion, $SO_2^{-\bullet}$. The peaks at −0.4 and −0.2 V are assigned to the oxidation of unsolvated and solvated $SO_2^{-\bullet}$, respectively. The peak appearing at 0.2 V is assigned to the oxidation of either $S_2O_4^{2-}$ or $S_2O_4^{-\bullet}$. The activation energy for the reduction of SO_2 in [C_4mim][NO_3] was measured to be 10 (±2) kJ mol^{-1} using chronoamperometric data at different temperatures. The stabilizing interaction of the solvent with the reduced species $SO_2^{-\bullet}$ leads to a different mechanism than that observed in conventional aprotic solvents. The high sensitivity of the system to SO_2 also suggests that [C_4mim][NO_3] may be a viable solvent in gas sensing applications.

1. Introduction

The term room-temperature ionic liquid (RTIL) describes a group of ionic compounds that are liquid at temperatures around 298 K and generally consist of a bulky, asymmetrical organic cation and a weakly coordinating inorganic anion. Wide electrochemical windows, negligible volatility, high thermal stability, and high intrinsic conductivity are properties intrinsic to RTILs as a group, making them potentially useful over a range of applications. Additionally, the properties of individual RTILs can be adjusted by changing the cation or anion, allowing an RTIL to be tuned for a specific purpose.[1−3] RTILs have been successfully used as solvents for organic,[4,5] enzymatic,[6] and inorganic[7] synthesis, as well as for separation purposes.[8] They have also been used as electrolytes in lithium batteries,[9] fuel cells,[10] and solar cells.[11]

Because of their aforementioned properties, RTILs have been investigated as solvents for electrochemical experiments in general and gas sensing in particular.[3] Although conventional solvents are frequently hampered by the ambient conditions of a gas sensing environment, drying out because of high volatility or degrading due to thermal instability, RTILs are not limited by these concerns.[3] High viscosity, another characteristic property of RTILs, results in slower response times than those obtained in more conventional solvents,[12] but electrochemical gas sensing using RTILs continues to be an active field of research. Much work in the field thus far has compared voltammetry observed in RTILs with that observed in conventional solvents in order to better understand the redox mechanism of the electroactive species under investigation. Frequently, as in the cases of nitrogen dioxide,[13] hydrogen,[14] and ammonia gas,[15] voltammetry obtained in RTILs shows features previously unseen in conventional solvents.

Sulfur dioxide is a major air pollutant that is released into the atmosphere from the combustion of sulfur-containing fuel, in both industrial and natural processes.[16,17] Though there is difficulty in assigning health effects to a single pollutant, sulfur dioxide has been linked to respiratory problems, particularly in asthmatics, as well as being thought to contribute to increased mortality.[18] Sulfur dioxide is also one of the major causes of acidic rain, and many countries have implemented plans to reduce sulfur dioxide emissions.[16,17,19,20] For this reason, sulfur dioxide gas sensors for industrial use have been researched extensively. There are many examples of electrochemical sulfur dioxide sensors in the literature,[21−24] and the reduction mechanism has been investigated in a range of different solvents.[21,25−28] Electrochemical methods of sulfur dioxide detection have the advantage of being cheap, rapid, and facile as compared to spectroscopic methods sometimes employed for the same purpose.

In nonaqueous solvents such as dimethylformamide (DMF) and dimethylsulphoxide (DMSO), the reduction of sulfur dioxide to the SO_2^- radical appears as a cyclic voltammetric feature.[26]

* Author to whom all correspondence should be addressed. E.mail: richard.compton@chem.ox.ac.uk. Tel: +44 (0) 1865 275 413. Fax: +44 (0) 1865 275 410.
[†] University of Oxford.
[‡] Queen's University Belfast.

10.1021/jp7109093 CCC: $40.75
Published on Web 02/13/2008

$$SO_2 + e^- \rightleftarrows SO_2^{-\bullet} \quad (1)$$

From two to four oxidative back peaks are observed, the first of which is most often assigned to the oxidation of the SO_2^- radical,[26−29] though in one case it was assigned decomposition products or impurities in the solvent (dimethylformamide).[30] There is disagreement in the literature as to the assignment of the other peaks. One possible reaction involves the dimerization of the SO_2^- radical to form the dithionite ion, which is then oxidized at the electrode surface.[27,29,30]

$$2\ SO_2^{-\bullet} \rightleftarrows S_2O_4^{2-} \quad (2)$$

$$S_2O_4^{2-} - 2e^- \rightleftarrows 2\ SO_2 \quad (3)$$

Another possibility is that a complex formed from sulfur dioxide and the SO_2^- radical is electrochemically oxidized.[28,30,31]

$$SO_2^{-\bullet} + SO_2 \rightleftarrows S_2O_4^{-\bullet} \quad (4)$$

Other processes have also been suggested, including the disproportionation of the SO_2^- radical into SO and SO_3^{2-} with subsequent oxidation of SO_3^{2-},[28]and the formation and oxidation of the complexes $S_3O_6^{2-}$ [27,31] and $S_4O_8^{2-}$.[26] Bruno et al. propose that dithionite can break down into SO_2 and SO_2^{2-} as an alternative to combining with SO_2 to create $S_3O_6^{2-}$.[27] This process is more likely to take precedence at lower concentrations and results in a new candidate species for oxidation, SO_2^{2-}.

The present work examines the reduction of sulfur dioxide in $[C_4mim][NO_3]$, $[C_2mim][NTf_2]$, $[C_4mim][BF_4]$, $[C_4mim][PF_6]$, and $[C_6mim][Cl]$ (see Figure 1 for structures) and compares the results to those obtained in conventional nonaqueous solvents. Focusing on the voltammetry of SO_2 reduction in $[C_4mim][NO_3]$ over a range of concentrations and temperatures reveals one peak on the cathodic sweep and up to four peaks on the anodic sweep. Peak assignments have been made based on the present experimental data and the literature data.

2. Experimental Section

2.1. Reagents and Instrumentation. 1-Butyl-3-methylimidazolium nitrate ($[C_4mim][NO_3]$),[13,32,33] 1-ethyl-3-methylimidazolium bis(trifluoromethylsufonyl)imide ($[C_2mim][NTf_2]$),[34] and 1-hexyl-3-methylimidazolium chloride ($[C_6mim][Cl]$)[34] were prepared following procedures reported in the literature. 1-Butyl-3-methylimidazolium tetrafluoroborate ($[C_4mim][BF_4]$, high purity) and 1-butyl-3-methylimidazolium hexafluorophosphate ($[C_4mim][PF_6]$, high purity) were kindly donated by Merck KGaA and used as received. Sulfur dioxide (BDH, 99.9%; CK Gas Products, 10.18% and 1.04% in N_2), ferrocene (Aldrich, 98%), tetrabutylammonium perchlorate (TBAP, Fluka, Puriss electrochemical grade, >99%), and acetronitrile (Fischer Scientific, dried and distilled, >99.99%) were used as received without further purification.

Cyclic voltammetry (CV) was performed using a type-II μAutolab (Eco Chemie, Utrecht, Netherlands), which was interfaced with a PC using GPES (version 4.9) software for Windows. Measurements were performed using a two-electrode cell consisting of a platinum working ultramicroelectrode (10 μm diameter) and a silver wire quasi-reference electrode (0.5 mm diameter). The electrodes were housed in a glass "T-cell" specially designed to control the environment of the RTIL.[35,36] The microelectrode was modified using a portion of a disposable plastic micropipette tip to create a reservoir in which 20 μL of ionic liquid was placed. The T-cell containing the ionic liquid was kept under vacuum for at least 90 min prior to taking any measurements. Sulfur dioxide from a gas cylinder was introduced into the cell via PTFE tubing through one arm of the T-cell and removed through the other. The gas was then directed into the fume cupboard, again via the nonreactive PTFE tubing. The system generally took 30−40 min after first introducing the gas to give a consistent voltammetric response.

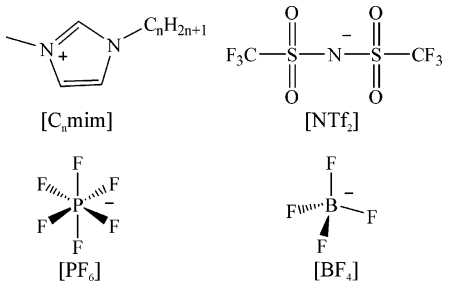

Figure 1. Molecular structures of anions and cations that comprise the RTILs examined in this work, and the notation used to describe them.

2.2. Electrode Preparation. Before use, the microelectrode was polished on soft lapping pads (Kemet Ltd., U.K.) using 1.0 and 0.3 μm aqueous alumina slurries (Buehler, IL). The radius of the microdisk electrode was electrochemically calibrated by analyzing the steady-state voltammetry of a 2 mM ferrocene solution in acetonitrile, which contained 0.1 M TBAP as a supporting electrolyte. The diffusion coefficient value used was 2.3×10^{-9} m^2 s^{-1} at 298 K.[37]

2.3. Chronoamperometric Experiments. Chronoamperometric transients were achieved using a sample time of 0.01 s. The pretreatment step consisted of holding the potential at 0 V for 20 s, followed by a 2 s equilibration period. The potential was stepped to the required value, and the current was measured for 10 s. The nonlinear curve fitting function in Origin 7.0 (MicroCal Software Inc.) following the Shoup and Szabo[38] approximation as employed by Evans et al.[39] was used to fit the experimental data. The equations used in this approximation describe the current response within an accuracy of 0.6% and are given below

$$I = -4nFDcr_d f(\tau) \quad (5)$$

$$f(\tau) = 0.7854 + 0.8863\tau^{-1/2} + 0.2146e^{-0.7823\tau^{-1/2}} \quad (6)$$

$$\tau = \frac{4Dt}{r_d^2} \quad (7)$$

where n is the number of electrons transferred, F is the Faraday constant, D is the diffusion coefficient, c is the bulk concentration of the parent species, r_d is the radius of the microdisk electrode, and t is the time.

The value of the electrode radius was fixed, having been calibrated previously. The software performed up to 100 iterations on the data, stopping when the experimental data had been optimized. A value for the diffusion coefficient, D, and the product of the number of electrons and the concentration of the parent species, nc, was thus obtained.

2.4. Temperature Control. Variable temperature experiments were carried out in a specially designed heated faraday cage[40] with a heating element from Arbor Electronics Ltd. (Essex, U.K.). Gas travelled through a PTFE coil heated to the same temperature as the rest of the box prior to entering the T-cell.

2.5. Modeling the Reduction of SO_2. Simulation of the reduction of SO_2 was carried out using the one-dimensional

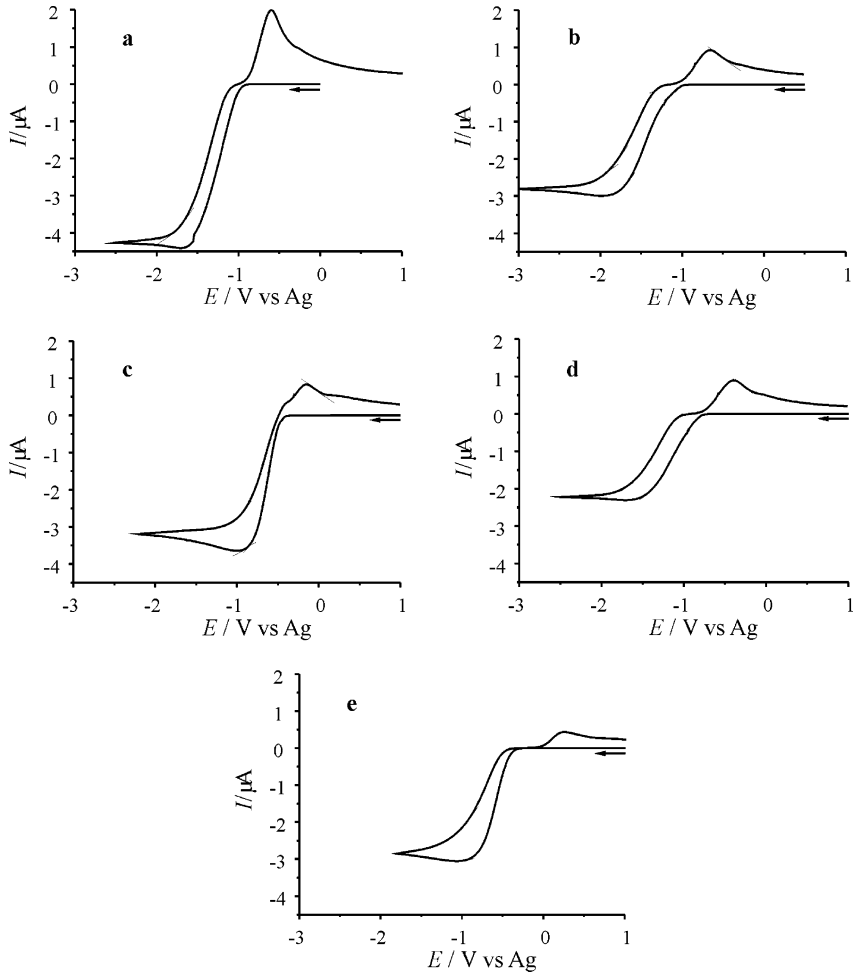

Figure 2. Cyclic voltammograms of the reduction of SO_2 on a 10-μm-diameter platinum electrode at a scan rate of 4 V s^{-1} in (a) [C_2mim][NTf_2], (b) [C_4mim][BF_4], (c) [C_4mim][NO_3], (d) [C_4mim][PF_6], and (e) [C_6mim][Cl].

digital simulation program DigiSim 3.03 (BAS Technicol).[41] The cyclic voltammogram of 100% SO_2 in [C_4mim][NO_3] obtained at a scan rate of 50 V s^{-1} and shown in Figure 3 was modeled using the hemispherical diffusion model. The following mechanism was used

$$A + e^- \rightleftarrows B \quad (8)$$

$$B \rightarrow C \quad (9)$$

$$C \rightleftarrows D + e^- \quad (10)$$

where A and D are SO_2, B is $SO_2^{-\bullet}$, and C is solvated $SO_2^{-\bullet}$.

3. Results and Discussion

3.1. Reduction of SO_2 in Various RTILs. The reduction of sulfur dioxide was examined in several different RTILs ([C_2mim][NTf_2], [C_4mim][BF_4], [C_4mim][NO_3], [C_4mim][PF_6], and [C_6mim][Cl]). Figure 2 shows the cyclic voltammetry (CV) of a saturated solution of SO_2 obtained at a scan rate of 4 V s^{-1} in each of the five ionic liquids on a 10-μm-diameter platinum electrode. The voltammograms are arranged in order of increasing viscosity of the ionic liquid: 34,[34] 112,[34] 266,[42] 371,[42] and 7453[43] cP, respectively (values determined at 20 °C). The variation in RTIL composition, which results in differing potential window sizes, precludes scanning over the same potential range for each RTIL, but the solutions were generally scanned from 1 V to a minimum of −3 V versus silver quasi-reference electrode. The cathodic peak appears between −2.0 and −1.0 V. This peak is attributed to the reduction of SO_2 to its radical anion, as described in eq 1. In conventional aprotic solvents, the peak is generally observed between −1.5 V versus ferricinium/ferrocene (in hexamethylphosphoramide)[26] and −0.7 V versus SCE (dimethylsulfoxide).[27] When the scan rate is increased from 0.05 V s^{-1}, the voltammetry goes from steady-

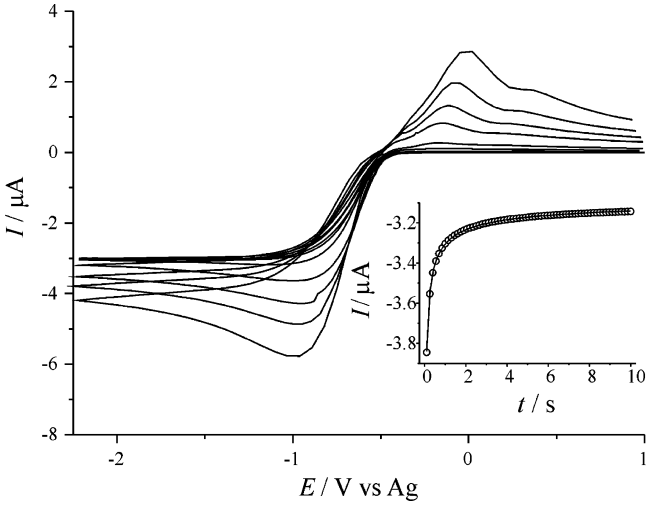

Figure 3. Cyclic voltammograms of the reduction of SO_2 on a 10-μm-diameter platinum electrode in [C_4mim][NO_3] at scan rates of 0.05, 0.1, 1, 2, 4, 8, 15, 30, and 50 V s^{-1}. The inset shows the experimental (○) and fitted theoretical (−) chronoamperometric transients for the reduction of SO_2. The potential was stepped from 0 to −1.5 V.

TABLE 1: Diffusion Coefficient and Solubility Values for SO_2 in Various RTILs[a]

RTIL	viscosity (cP)	diffusion coefficient (D) ($m^2\ s^{-1}$)	solubility ($P_{SO_2} = 1$ atm) (mM)	D*solubility (m^2 mM s^{-1})
$[C_2mim][NTf_2]$	34 [34]	$8.7\ (\pm0.3) \times 10^{-9}$	230 ($\pm$7)	2.0×10^{-6}
$[C_4mim][BF_4]$	112 [34]	$7.9\ (\pm0.4) \times 10^{-10}$	1600 ($\pm$100)	1.3×10^{-6}
$[C_4mim][NO_3]$	266 [42]	$4.8\ (\pm0.5) \times 10^{-10}$	3000 ($\pm$420)	1.4×10^{-6}
$[C_4mim][PF_6]$	371 [42]	$4.4\ (\pm0.2) \times 10^{-9}$	250 ($\pm$9)	1.1×10^{-6}
$[C_6mim][Cl]$	7453 [43]	$3.1\ (\pm0.1) \times 10^{-10}$	3500 ($\pm$66)	1.1×10^{-6}

[a] All viscosity data taken at 20 °C.

state to transient-shaped in all RTILs. Steady-state behavior is not always observed on microelectrodes in RTILs because the low diffusion coefficients associated with those solvents make planar diffusion the dominant form of mass transport until sufficiently slow scan rates produce edge effects.[44] However, gases have relatively high diffusion coefficients as compared to solid species, which causes steady-state behavior to be observed in the reduction of SO_2 at higher scan rates than usual for solid species in RTILs. A true steady-state response obeys the following inequality[44]

$$\nu \ll \frac{RTD}{nFr_d^2} \tag{11}$$

where ν is the scan rate, R is the universal gas constant, and T is the absolute temperature. The radius of the electrode, r_d, is taken as 5.24 μm, and the diffusion coefficient, D, varies with ionic liquid as discussed in the following paragraph.

Potential step experiments were performed on the cathodic wave in order to calculate the solubility and diffusion coefficient of SO_2 in each of the RTILs. The potential was stepped from 0 V to a potential past that at which the signal reached steady state (e.g., -1.5 V in $[C_4mim][NO_3]$), and the current was measured for 10 s. A chronoamperometric transient obtained in $[C_4mim][NO_3]$ is shown in the inset of Figure 3, the experimental data represented by open dots and the theoretically fitted data represented by a solid line. The experimental data were fitted to the Shoup and Szabo[38] expression, and the compiled diffusion coefficient and solubility data (assuming a one-electron process) can be found in Table 1. No trends in solubility or diffusion coefficient are observed with respect to viscosity in these systems, though other systems sometimes exhibit an inverse linear relationship between diffusion coefficient and solvent viscosity as described by the Stokes−Einstein equation.[45] SO_2 appears to be the most soluble in $[C_6mim][Cl]$, a fact seemingly at odds with the comparatively low current response observed for that RTIL in Figure 2. However, a particularly low diffusion coefficient in that RTIL prevents the diffusion layer from being replenished with SO_2 quickly enough to produce a large response even when the solution has a high concentration of SO_2 overall. Thus, the high solubility of SO_2 in $[C_6mim][Cl]$ (3500 mM) is mitigated by its comparatively low diffusion coefficient (3.1×10^{-10} $m^2\ s^{-1}$). This effect can be evaluated by multiplying the solubility and diffusion coefficient as in the fifth column of Table 1. A comparison of those values suggests that SO_2 in $[C_2mim][NTf_2]$ should show the largest cathodic response at a microelectrode despite relatively low solubility, a prediction confirmed by the voltammetry given in Figure 2.

At least two peaks are observed on the reverse sweep in all of the RTILs, and the voltammetry obtained in each RTIL is similar in appearance to that obtained in each of the others. A prominent back peak is followed by a broad shoulder of lesser intensity on the reductive sweep. Close examination of the voltammetry obtained in $[C_4mim][NO_3]$ reveals a third peak, a shoulder at more negative potentials than the prominent peak. The shoulder peak that appears at less negative potentials is also more easily observed in $[C_4mim][NO_3]$ than in the other RTILs. Because of the well-defined and unique voltammetry, high solubility, and low diffusion coefficient of SO_2 in $[C_4mim][NO_3]$, that RTIL was chosen to carry out further studies on the mechanism of SO_2 reduction.

3.2. Reduction of SO_2 in $[C_4mim][NO_3]$. Figure 3 shows the reduction of a saturated solution of SO_2 in $[C_4mim][NO_3]$ at a range of scan rates from 0.5 to 50 V s^{-1}. As the scan rate increases, the cathodic peak shifts to more negative potentials while the anodic back peaks shift to less negative potentials. A plot of the peak current versus the square root of the scan rate does not go through the origin for any of the observed peaks. This indicates that although the peaks are diffusion-limited the species involved are at the switchover between linear and convergent diffusion. At 4 V s^{-1}, the anodic peaks a through c appear at -0.4, -0.2, and 0.2 V, respectively, as shown in Figure 4. Generally, at scan rates below 1 V s^{-1}, only peaks b and c are observed. In some cases, at intermediate scan rates (between 1 and 15 V s^{-1}), a fourth peak is observed at -0.3 V. This peak is designated peak a′, and can be seen in the inset of Figure 4.

To assist in the assignment of the anodic peaks observed on the reverse scan, we took voltammetry of 10 and 1% SO_2 in nitrogen in $[C_4mim][NO_3]$. Comparison of the voltammograms obtained at these concentrations versus those obtained using 100% SO_2 shows all peaks shifting to more negative potentials as the concentration increases. This effect could be caused by change to the quasi-reference electrode as SO_2 coats the silver wire. Peak b is the most prominent peak on the reverse scans in both of the lower concentrations. Peak c also appears in both low-concentration mixtures at very high scan rates (30 V s^{-1}). Chronoamperometric transients, obtained by the same method as that described in the previous section, showed an average solubility of 2100 $\pm$ 290 mM for 10% SO_2 and 340 $\pm$ 18 mM for 1% SO_2. The diffusion coefficients were found to be $8.1 \pm 1.9 \times 10^{-11}$ $m^2\ s^{-1}$ and $7.3 \pm 0.4 \times 10^{-11}$ $m^2\ s^{-1}$, respectively. At higher concentrations the current response did not scale with concentration, probably because the high SO_2 solubility leads to the electrode process becoming unsupported.

Literature sources are inconsistent in their assignments of the oxidative back peaks observed in conventional aprotic solvents, though almost all agree that the first back peak (peak a, Figure 4) represents the oxidation of the radical anion $SO_2^{-\bullet}$, the product of the direct reduction of SO_2.[26−28] In $[C_4mim][NO_3]$, this assignment is supported by the appearance of peak a as the scan rate increases. Because $SO_2^{-\bullet}$ is a very reactive species, the scan rate must be faster than the rate of the chemical processes that the radical anion undergoes if this peak is to be seen. Notably, the dimerization of the anion radical to form dithionite, $S_2O_4^{2-}$ and the reaction of the anion radical with the parent species to form $S_2O_4^{-\bullet}$ take place quickly, However,

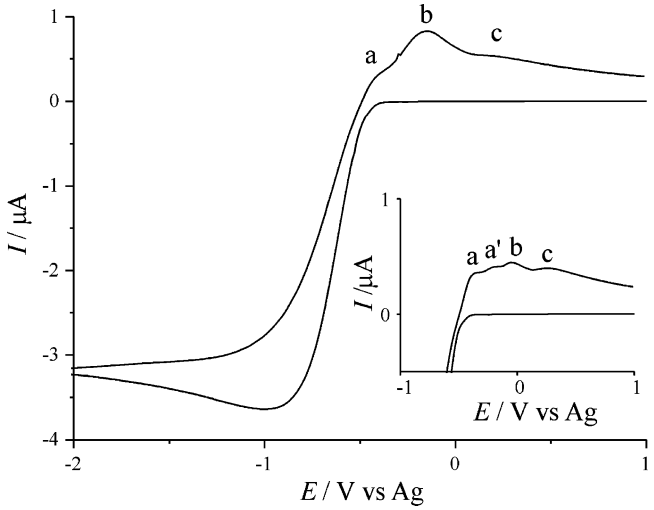

Figure 4. Typical cyclic voltammogram of the reduction of SO_2 on a 10-μm-diameter platinum electrode in [C_4mim][NO_3] at a scan rate of 4 V s^{-1}. The inset shows the appearance of a fourth peak in a reverse wave of a voltammogram taken of the same process at the same scan rate.

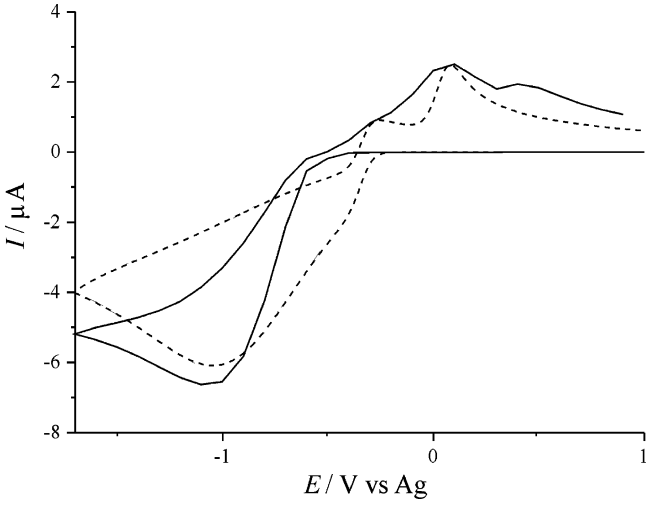

Figure 5. Comparison of experimental (solid line) and simulated (dashed line) cyclic voltammograms at a scan rate of 50 V s^{-1}, obtained from the generic scheme given by eqs 8−10. The simulated voltammogram was generated using the following parameters: E_f^0 ($SO_2/SO_2^{-\bullet}$ unsolvated) −0.5 V, α ($SO_2/SO_2^{-\bullet}$ unsolvated) 0.1, k_0 ($SO_2/SO_2^{-\bullet}$ unsolvated) 3×10^{-4} cm s^{-1}, E_f^0 ($SO_2/SO_2^{-\bullet}$ solvated) 0.05 V, α ($SO_2/SO_2^{-\bullet}$ solvated) 0.5, k_0 ($SO_2/SO_2^{-\bullet}$ solvated) 0.1 cm s^{-1}.

peak b, which appears in all ionic liquids tested, is also a good candidate for the oxidation of $SO_2^{-\bullet}$.

A recent article by Choi et al. discusses the stabilizing effect of the acidic C2 proton in imidazolium-based ionic liquids.[46] Specifically, the stabilization of oxygen anion radicals was observed. Positing that a similar stabilizing interaction occurs between the sulfur dioxide anion radical and the ionic liquids tested, peak b is assigned to the oxidation of solvated $SO_2^{-\bullet}$. This assignment is consonant with the presence of peak b in the voltammetry of all RTIL/SO_2 systems observed. The peak position indicates that the stabilization of the anion radical increases the potential necessary to oxidize solvated $SO_2^{-\bullet}$. The presence of peak b and absence of peak a in low SO_2 concentration solutions suggests that the greater ratio of solvent to sulfur dioxide anion radical results in complete solvation of the radical. Even at scan rates as high as 50 V s^{-1}, peak a is absent from 1 and 10% SO_2 systems.

In order to support or disprove this proposed interaction of the imidazolium RTIL and the anion radical, we modeled the system using DigiSim.[41] This qualitatively confirmed a mechanism of the following type:

$$SO_2 + e^- \overset{k_0}{\rightleftharpoons} SO_2^{-\bullet} \tag{12}$$

$$SO_2^{-\bullet} + \text{solvent} \overset{k_f}{\rightarrow} SO_2^{-\bullet}\cdots\text{solvent} \tag{13}$$

$$SO_2^{-\bullet}\cdots\text{solvent} \overset{k_0}{\rightleftharpoons} SO_2 + e^- \tag{14}$$

Figure 5 shows a simulated cyclic voltammogram overlaid on a cyclic voltammogram obtained experimentally (50 V s^{-1}, 100% SO_2). E_f^0 ($SO_2/SO_2^{-\bullet}$ unsolvated) was determined to be −0.5 V, and a low α value (∼0.1) was needed to broaden the cathodic peak. The reduction of SO_2 was found to have quasi-reversible electrode kinetics, with a k_0 of $\sim 3 \times 10^{-4}$ cm s^{-1}. E_f^0 ($SO_2/SO_2^{-\bullet}$ solvated) was determined to be 0.05 V, with an α value of 0.5 and a k_0 of ∼0.1 cm s^{-1}. The EC mechanism had fast follow-up kinetics. The simulated cyclic voltammetry supports the assignment of peak a to unsolvated $SO_2^{-\bullet}$ and peak b to solvated $SO_2^{-\bullet}$.

Peak c is likely due to the oxidation of either the dithionite ion, $S_2O_4^{2-}$, formed by dimerization of $SO_2^{-\bullet}$, or the $S_2O_4^{-\bullet}$ radical anion formed by reaction of $SO_2^{-\bullet}$ with the parent molecule. Literature sources agree that these two species are common products of chemical reactions stemming from the reduction of SO_2.[26,27,29,30,47] Generally, dithionite is the more prevalent form, especially in DMSO.[27,47] In DMF, however, the equilibrium between $SO_2^{-\bullet}$ and its dimer shifts to the left, leaving some $SO_2^{-\bullet}$ available for complexation with SO_2.[27,30] Though the $S_2O_4^{-\bullet}$ complex is not always voltammetrically observed in conventional aprotic solvents,[28,29,47] it is possible that it could be stabilized by interaction with the acidic C2 proton of the ionic liquid in the same manner as the monomeric radical anion is stabilized by the RTIL. This stabilization would lead to an observable signal, which is why this complex is considered a candidate for peak c.

Potteau et al. dispute the assignation of dithionite, the other candidate species for peak c, to any cyclic voltammetric feature in conventional solvents, claiming that dithionite is nonelectroactive.[48] Their assertion is backed by spectroscopic studies that show the presence of dithionite in a solution of hexamethylphosphoramide (HMPA) for which no redox peak is observed.[48] Although this observation may be pertinent to the reduction of SO_2 in HMPA, the electrochemical response of $Na_2S_2O_4$ was demonstrated in DMSO by Bruno et al., indicating that dithionite is not intrinsically nonelectroactive.[27]

The appearance of peak a′ is sporadic enough to make assignment difficult to the point of impossible. It is possible that if peak c is due to a stabilized radical anion complex, $S_2O_4^{-\bullet}$, that peak a′ could be the oxidation of the corresponding unsolvated species; however, no evidence directly supports this conclusion.

3.3. Effect of Heating on the Reduction of SO_2 in [C_4mim][NO_3]. Heating a cell consisting of SO_2 and 20 μL [C_4mim][NO_3] from ambient temperature (23 °C) to 35 °C in a specially designed temperature-controlled faraday cage produced interesting changes in the voltammetry observed. As was stated in the previous section, low scan rate voltammograms of 100% SO_2 show only peaks b and c. Peaks a and a′ appear above a threshold scan rate. Voltammograms taken at ambient temper-

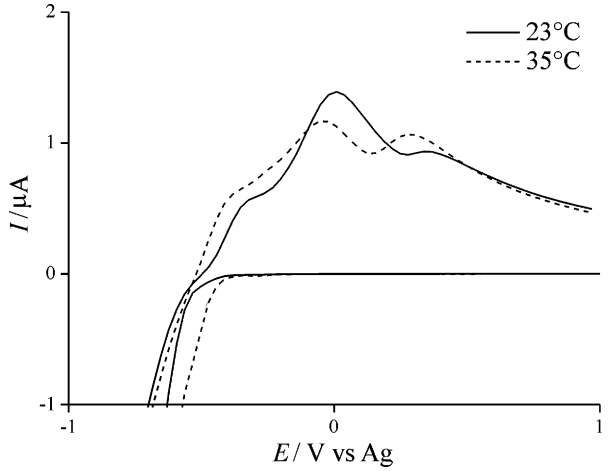

Figure 6. Comparison of the reverse waves of cyclic voltammograms of the reduction of SO_2 on a 10-μm-diameter platinum electrode in [C_4mim][NO_3] at a scan rate of 15 V s^{-1} at 23 and 35 °C.

ature showed that the threshold from two peaks (peaks b and c) to three or four peaks (peaks a and a′) occurred at faster scan rates than those scan rates at which the same transition occurred at 35 °C. This observation suggests that the species responsible for those two peaks are present in higher concentrations at higher temperatures. In the case of peak a, adding heat to the system stabilizes unsolvated $SO_2^{-\bullet}$, resulting in the presence of more unsolvated $SO_2^{-\bullet}$ in solution.

Figure 6 shows a comparison of the anodic peaks at 23 and 35 °C at a scan rate of 15 V s^{-1}. All peaks have shifted to more reducing potentials. Peak c has increased in intensity, and peak b has decreased. The inverse relationship of peaks b and c could be due to competition for solvent molecules between $SO_2^{-\bullet}$ and $S_2O_4^{-\bullet}$ if peak c is caused by the oxidation of the solvated radical complex. This inverse relationship could also be explained by the aforementioned greater stability of unsolvated $SO_2^{-\bullet}$ in the heated solution, leading to increased dimerization of that species to dithionite.

Chronoamperometric data shows a decrease in concentration of SO_2 as the temperature increases. Chronoamperometric transients also yielded data on the relationship between the diffusion coefficient of SO_2 and temperature. Data taken at 23, 27, 31, and 35 °C show an increase in diffusion coefficient as the temperature increases. An Arrhenius plot was constructed, and the diffusional activation energy of SO_2 in [C_4mim][NO_3] was calculated to be 10 (±2) kJ mol^{-1}. The activation energy of viscosity was reported to be 38.3 kJ mol^{-1}.[42] This discrepancy is consistent with the previously observed lack of a consistent relationship between diffusion coefficient of SO_2 and solvent viscosity in this system.

4. Conclusions

The electrochemical reduction of sulfur dioxide on a 10 μm platinum electrode in several different RTILs has been studied, with special attention paid to the reduction of SO_2 in [C_4mim][NO_3]. At high concentrations of SO_2, one cathodic wave is observed and assigned to the reduction of SO_2 to $SO_2^{-\bullet}$. In [C_4mim][NO_3], that reduction peak appears at −1.0 V. Two anodic waves are observed in all of the ionic liquids studied at a scan rate of 4 V s^{-1}. A third anodic peak was observed only in [C_4mim][NO_3]. The high solubility (3000 (±420) mM) and relatively high diffusion coefficient (4.8 (±0.5) × 10^{-10} m^2 s^{-1}) of SO_2 in [C_4mim][NO_3] as well as the third anodic feature observed made the reduction of SO_2 in [C_4mim][NO_3] the focus of further study. The anodic peaks appear at −0.4, −0.2, and 0.2 V and are labeled peaks a through c, respectively. A fourth peak is sometimes observed at −0.3 V and is labeled peak a′. Peaks a and b are assigned to the oxidation of unsolvated and solvated $SO_2^{-\bullet}$, respectively. Interaction with the acidic C2 proton of the imidazolium cation stabilizes $SO_2^{-\bullet}$, leading to two distinct peaks for the stabilized and unstabilized species. Peak c is assigned to the oxidation of either $S_2O_4^{2-}$ or $S_2O_4^{-\bullet}$, and peak a′ is unassigned because of its transient nature. Study of the same system at different temperatures resulted in an approximation of the activation energy for the reduction of SO_2 in [C_4mim][NO_3] (10 (±2) kJ mol^{-1}). The voltammetry of SO_2 observed in [C_4mim][NO_3] loosely resembles that obtained in conventional aprotic solvents. However, the stabilizing interaction of the solvent with the reduced species leads to a different mechanism than that observed in conventional solvents. The high sensitivity of the system to SO_2 also suggests that [C_4mim][NO_3] may be a viable solvent in gas sensing applications.

Acknowledgment. We thank the following for financial support: Physical and Theoretical Chemistry Laboratory (L.E.B.A.), Schlumberger Cambridge Research (D.S.S.), and the Department of Education and Learning in Northern Ireland and Merck GmBH (L.A.).

References and Notes

(1) Ohno, H. *Bull. Chem. Soc. Jpn.* **2006**, *79*, 1665.
(2) Buzzeo, M. C.; Evans, R. G.; Compton, R. G. *ChemPhysChem* **2004**, *5*, 1106.
(3) Silvester, D. S.; Compton, R. G. *Z. Phys. Chem.* **2006**, *220*, 1247.
(4) Vidiš, A.; Laurenczy, G.; Küsters, E.; Sedelmeier, G.; Dyson, P. J. *J. Phys. Org. Chem.* **2007**, *20*, 109.
(5) D'Anna, F.; Frenna, V.; Noto, R.; Pace, V.; Spinelli, D. *J. Org. Chem.* **2006**, *71*, 9637.
(6) Raab, T.; Bel-Rhlid, R.; Williamson, G.; Hansen, C.-E.; Chaillot, D. *J. Mol. Catal. B: Enzym.* **2007**, *44*, 60.
(7) Xue, X.; Liu, C.; Lu, T.; Xing, W. *Fuel Cells* **2006**, *6*, 347.
(8) Yokozeki, A.; Shiflett, M. B. *Appl. Energy* **2007**, *84*, 351.
(9) Howlett, P. C.; MacFarlane, D. R.; Hollenkamp, A. F. *Electrochem. Solid-State Lett.* **2004**, *7*, A97.
(10) de Souza, R. F.; Padilha, J. C.; Gonçalves, R. S.; Dupont, J. *J. Electrochem. Commun.* **2003**, *5*, 728.
(11) Papageorgiou, N.; Athanassov, Y.; Armand, M.; Bonhôte, P.; Pettersson, H.; Azam, A.; Grätzel, M. *J. Electrochem. Soc.* **1996**, *143*, 3099.
(12) Buzzeo, M. C.; Hardacre, C.; Compton, R. G. *Anal. Chem.* **2004**, *76*, 4583.
(13) Broder, T. L.; Silvester, D. S.; Aldous, L.; Hardacre, C.; Compton, R. G. *J. Phys. Chem. B* **2007**, *111*, 7778.
(14) Silvester, D. S.; Aldous, L.; Hardacre, C.; Compton, R. G. *J. Phys. Chem. B* **2007**, *111*, 5000.
(15) Ji, X.; Silvester, D. S.; Aldous, L.; Hardacre, C.; Compton, R. G. *J. Phys. Chem. C*, in press.
(16) Hall, J.; Tipping, E.; Sutton, M.; Dragosits, U.; Evans, C.; Foot, J.; Harriman, R.; Monteith, D.; Broadmeadow, M.; Langan, S.; Helliwell, R.; Whyatt, D.; Lee, D.; Curtis, C. Transboundary Air Pollution: Acidification, Eutrophication and Ground-Level Ozone in the UK; National Expert Group on Transboundary Air Pollution, 2001.
(17) NEGTAP. Transboundary Air Pollution: Acidification, Eutrophication and Ground-Level Ozone in the UK; National Expert Group on Transboundary Air Pollution, 2001.
(18) WHO. WHO Air quality guidelines for particulate matter, ozone, nitrogen dioxide and sulfur dioxide; World Health Organization, 2006.
(19) Carmichael, G. R.; Streets, D. G.; Calori, G.; Amann, M.; Jacobson, M. Z.; Hansen, J.; Ueda, H. *Environ. Sci. Technol.* **2002**, *36*, 4707.
(20) Chestnut, L. G.; Mills, D. M. *J. Environ. Manage.* **2005**, *77*, 252.
(21) Cai, Q.; Xian, Y.-z.; Li, H.; Zhang, Y.-m.; Tang, J.; Jin, L.-t. *Huadong Shifan Daxue Xuebao, Ziran Kexueban* **2001**, *3*, 57.
(22) Hodgson, A. W. E.; Jacquinot, P.; Hauser, P. C. *Anal. Chem.* **1999**, *71*, 2831.
(23) Skeaff, J. M.; Bubreuil, A. A. *Sens. Actuators, B* **1993**, *10*, 161.
(24) Gauthier, M.; Chamberland, A. *J. Electrochem. Soc.* **1977**, *124*, 1579.
(25) Neta, P.; Huie, R. E.; Harriman, A. *J. Phys. Chem.* **1987**, *91*, 1606.
(26) Potteau, E.; Levillain, E.; Lelieur, J.-P. *J. Electroanal. Chem.* **1999**, *476*, 15.

(27) Bruno, P.; Caselli, M.; Traini, A. *J. Electroanal. Chem.* **1980**, *113*, 99.
(28) Gardner, C. L.; Fouchard, D. T.; Fawcett, W. R. *J. Electrochem. Soc.* **1981**, *128*, 2345.
(29) Magno, F.; Mazzocchin, G. A.; Bontempelli, G. *Electroanal. Chem. Interfacial Electrochem.* **1974**, *57*, 89.
(30) Martin, R. P.; Sawyer, D. T. *Inorg. Chem.* **1972**, *11*, 2644.
(31) Kim, B.-S.; Park, S.-M. *J. Electrochem. Soc.* **1995**, *142*, 26.
(32) Cammarata, L.; Kazarian, S. G.; Salter, P. A.; Welton, T. *Phys. Chem. Chem. Phys.* **2001**, *3*, 5192.
(33) Broder, T. L.; Silvester, D. S.; Aldous, L.; Hardacre, C.; Crossley, A.; Compton, R. G. *New J. Chem.* **2007**, *31*, 966.
(34) Bonhôte, P.; Dias, A.-P.; Papageorgiou, N.; Kalyanasundaram, K.; Grätzel, M. *Inorg. Chem.* **1996**, *35*, 1168.
(35) Schroder, U.; Wadhawan, J. D.; Compton, R. G.; Marken, F.; Suarez, P. A. Z.; Consorti, C. S.; de Souza, R. F.; Dupont, J. *New J. Chem.* **2000**, *24*, 1009.
(36) Silvester, D. S.; Wain, A. J.; Aldous, L.; Hardacre, C.; Compton, R. G. *Electroanal. Chem.* **2006**, *596*, 131.
(37) Sharp, M. *Electrochim. Acta* **1983**, *28*, 301.
(38) Shoup, D.; Szabo, A. *J. Electroanal. Chem.* **1982**, *140*, 237.
(39) Evans, R. G.; Klymenko, O. V.; Saddoughi, S. A.; Hardacre, C.; Compton, R. G. *J. Phys. Chem. B* **2004**, *108*, 7878.
(40) Evans, R. G.; Klymenko, O. V.; Price, P. D.; Davies, S. G.; Hardacre, C.; Compton, R. G. *ChemPhysChem* **2005**, *6*, 526.
(41) Rudolph, M.; Reddy, D. P. *Anal. Chem.* **1994**, *66*, 589.
(42) Seddon, K. R.; Stark, A.; Torres, M.-J. *ACS Symp. Ser.* **2002**, *819*, 34.
(43) Ignat'ev, N. V.; Welz-Biermann, U.; Kucheryna, A.; Bissky, G.; Willner, H. *J. Fluorine Chem.* **2005**, *126*, 1150.
(44) Evans, R. G.; Klymenko, O. V.; Hardacre, C.; Seddon, K. R.; Compton, R. G. *J. Electroanal. Chem.* **2003**, *556*.
(45) Evans, R. G.; Wain, A. J.; Hardacre, C.; Compton, R. G. *ChemPhysChem* **2005**, *6*, 1035.
(46) Choi, D. S.; Kim, D. H.; Shin, U. S.; Deshmukh, R. R.; Lee, S.; Song, C. E. *Chem. Commun.* **2007**, 3467.
(47) Gardner, C. L.; Fouchard, D. T.; Fawcett, W. R. *J. Electrochem. Soc.* **1981**, *128*, 2337.
(48) Potteau, E.; Levillain, E.; Lelieur, J. P. *J. Electroanal. Chem.* **1997**, *436*, 271.